Modeling benzene plume elongation mechanisms exerted by ethanol using RT3D with a general substrate interaction module

Diego E. Gomez,[1] Phillip C. de Blanc,[2] William G. Rixey,[3] Phillip B. Bedient,[1] and Pedro J. J. Alvarez[1]

Received 18 May 2007; revised 28 January 2008; accepted 11 February 2008; published 8 May 2008.

[1] A mathematical model was developed to evaluate the effect of the common fuel additive ethanol on benzene fate and transport in fuel-contaminated groundwater and to discern the most influential benzene plume elongation mechanisms. The model, developed as a module for the Reactive Transport in 3 Dimensions (RT3D) model, includes commonly considered fate and transport processes (advection, dispersion, adsorption, biodegradation, and depletion of molecular oxygen during biodegradation) and substrate interactions previously not considered (e.g., a decrease in the specific benzene utilization rate due to metabolic flux dilution and/or catabolite repression) as well as microbial population shifts. Benzene plume elongation predictions, based on literature model parameters, were on the order of 40% for a constant source of E10 gasoline (10% vol/vol ethanol), which compares favorably to field observations. For low benzene concentrations (<1 mg/L), oxygen depletion during ethanol degradation was the principal mechanism hindering benzene natural attenuation. For higher benzene concentrations (exerting an oxygen demand higher than the available dissolved oxygen), metabolic flux dilution was the dominant plume elongation process. If oxygen were not limiting, as might be the case in zones undergoing aerobic biostimulation, model simulations showed that microbial growth on ethanol could offset negative substrate interactions and enhance benzene degradation, resulting in shorter plumes than baseline conditions without ethanol.

Citation: Gomez, D. E., P. C. de Blanc, W. G. Rixey, P. B. Bedient, and P. J. J. Alvarez (2008), Modeling benzene plume elongation mechanisms exerted by ethanol using RT3D with a general substrate interaction module, *Water Resour. Res.*, *44*, W05405, doi:10.1029/2007WR006184.

1. Introduction

[2] Ethanol, a substitute for the oxygenate methyl-*tert*-butyl ether (MTBE), is being increasingly used to meet renewable fuel and Clean Air Act requirements. The widespread use of ethanol in gasoline has led to an increase in its potential presence in groundwater contaminated with other fuel constituents such as benzene, toluene, ethylbenzene, and xylenes (BTEX). Preferential degradation of ethanol, including accelerated depletion of oxygen that otherwise would be available for bioremediation, has been reported to hinder BTEX degradation [*Corseuil et al.*, 1998; *Hunt et al.*, 1997; *Da Silva and Alvarez*, 2002; *Capiro et al.*, 2007]. As a result, longer BTEX plumes may form [*Ruiz-Aguilar et al.*, 2002], increasing the risk of exposure for potential downgradient receptors [*Powers et al.*, 2001a].

[3] A statistical analysis of benzene plumes from regular versus E10 gasoline (i.e., a blend with 10% vol/vol ethanol/gasoline) showed that mean benzene plume lengths were significantly longer ($p < 0.001$, as established by a Kruskal-Wallis rank test) when ethanol was present (i.e., 193 ± 135 ft for regular gasoline versus 263 ± 103 ft for E10, or 36% longer on a mean basis) [*Ruiz-Aguilar et al.*, 2003]. This is of particular concern because benzene is the most toxic of the monoaromatic hydrocarbons and its presence in fuel-contaminated sites often determines the need for remedial action. However, many confounding factors that influence plume length could not be considered because of data limitations (e.g., age and amount of spill, hydraulic conductivity, redox conditions). Thus, considerable uncertainty remains about the magnitude of the plume elongating effect of ethanol. Furthermore, the relative influence of different substrate interactions and geochemical footprints resulting from the presence of ethanol has not been investigated.

[4] Previous modeling efforts have simulated the effect of ethanol in E10 on benzene plume length. These models have typically considered important fate and transport processes that form the basis for our work, such as advection, dispersion, sorption, aerobic and anaerobic biodegradation, and ethanol-driven O_2 depletion. *Heermann and Powers*

[1]Department of Civil and Environmental Engineering, Rice University, Houston, Texas, USA.
[2]GSI Environmental, Inc., Houston, Texas, USA.
[3]Department of Civil and Environmental Engineering, University of Houston, Houston, Texas, USA.

0043-1397/08/2007WR006184$09.00

[1996] considered 2-D transport, with focus on cosolvency and mass transfer effects, and obtained a 10% increase in the length of a simulated *m*-xylene plume. *McNab et al.* [1999] considered 3-D aqueous transport from a finite source release zone and assumed that no anaerobic benzene degradation would occur following oxygen depletion exerted by ethanol, which resulted in a benzene plume elongation on the order of 100%. *Molson et al.* [2002], considered 3-D transport and microbial growth following Monod kinetics, including competition for oxygen between ethanol and hydrocarbon degraders. These simulations showed benzene plume elongation of up to 150%.

[5] Although past models provided valuable insight into how ethanol influences hydrocarbon plume dynamics, including competitive inhibition processes [*Lu et al.*, 1999], most have not simulated potentially important substrate interactions that influence catabolic enzyme induction (i.e., the synthesis of an enzyme by the cell, when in the presence of a specific substrate) and the metabolic flux of the target pollutants (i.e., the rate at which a pollutant such as benzene is metabolized per unit of biomass, which is analogous to the specific utilization rate). These interactions can cause slower BTEX degradation rates at sites with high ethanol concentrations [*Lovanh and Alvarez*, 2004], although this negative effect can be offset by higher microbial concentrations resulting from the presence of ethanol as an additional substrate [*Lovanh et al.*, 2002].

[6] This paper evaluates the importance of substrate interactions (benzene/ethanol) and the resulting microbial metabolic and population shifts that influence the natural attenuation of E10 releases and the resulting benzene plume length. An advanced computer module, designated the ''General Substrate Interaction Module'' (GSIM), was developed for this purpose for use with the Reactive Transport in 3 Dimensions (RT3D) model [*Clement et al.*, 1998]. Three mechanisms were considered separately and simultaneously to evaluate their relative importance on benzene plume elongation, under both constant and decreasing source scenarios. These mechanisms are (1) metabolic flux dilution (MFD), which is defined as a decrease in the specific benzene utilization rate due to noncompetitive inhibition when ethanol is present [*Lovanh and Alvarez*, 2004]; (2) catabolite repression, which is defined as the repression of inducible enzymes that degrade the target pollutant (e.g., benzene) by the presence of a preferred carbon source (e.g., ethanol) [*Madigan et al.*, 2000]; and (3) proliferation of different microbial populations in response to changes in oxygen and substrate availability.

2. Model Development

2.1. Contaminant Partitioning and Transport

[7] Contaminant advection, dispersion and adsorption to aquifer material were simulated using existing models, Reactive Transport in 3 Dimensions (RT3D) [*Clement et al.*, 1998] and the USGS flow model Modular Three-Dimensional Finite Difference Groundwater Flow (MODFLOW) model [*Harbaugh et al.*, 2000]. RT3D describes reactive flow and transport of multiple mobile and/or immobile species by solving the 3-D reactive advection-dispersion equation that governs these processes:

$$\frac{\partial C}{\partial t} = \left[D_x \frac{\partial^2 C}{\partial x^2} + D_y \frac{\partial^2 C}{\partial y^2} + D_z \frac{\partial^2 C}{\partial z^2}\right] - \left[\bar{v}_x \frac{\partial C}{\partial x} + \bar{v}_y \frac{\partial C}{\partial y} + \bar{v}_z \frac{\partial C}{\partial z}\right] + r \quad (1)$$

where D_i is the coefficient of hydrodynamic dispersion along the i axis (m^2/d), C is the contaminant aqueous-phase concentration (mg/L), $\bar{v}_i$ is the seepage velocity along the i axis (m/d), and r are all the reactions that occur in the aqueous and solid phases (mg/L d).

[8] RT3D uses the solvers for advection and dispersion from the 1997 Department of Defense version of MT3D, and requires MODFLOW to compute variations in groundwater head distribution (groundwater flow). It is a generalized multispecies version of the U.S. Environmental Protection Agency (EPA) transport code, MT3D [*Zheng*, 1990].The transport equation considers changes in concentration due to advection (water flow), dispersion, molecular diffusion, and external sources/sinks and reactions on the water/solid phase. GSIM calculates the value of the reaction term r explicitly, for each time step of the model, using a time-splitting approach. RT3D has been previously validated by comparing the code results against various numerical and analytical solutions [*Clement et al.*, 2000; *Sun and Clement*, 1999; *Sun et al. 1998*].

2.2. Substrate Interactions and Biodegradation

[9] One of the main advantages of RT3D is that it has a user-defined reaction option that can be used to simulate any type of user-specified reaction kinetics [*Clement et al.*, 1998]. This capability allows the development of custom biodegradation reaction modules without changing the coded flow and transport processes.

[10] A unique feature of the GSIM biodegradation module for RT3D is that it incorporates metabolic flux dilution (MFD) and catabolite repression (CR) (Figure 1). The metabolic flux of a compound is defined as the rate at which it is metabolized per unit biomass. Therefore, the specific substrate utilization rate (i.e., the degradation rate per unit biomass, U (g substrate g cells^{-1} h^{-1}), is a direct measure of metabolic flux. Metabolic flux dilution is a form of noncompetitive inhibition that decreases the specific rate of utilization of one substrate because of the utilization of another substrate [*Lovanh and Alvarez*, 2004]. Previous laboratory studies have shown that the metabolic flux of a compound in a mixture is proportional to its relative availability, expressed as a fraction of the available organic carbon [*Egli et al.*, 1993; *Lovanh et al.*, 2002].

[11] Ethanol may also act as a cosolvent, increasing BTEX mobility [*Groves*, 1988]. Cosolvency, however, is not considered in this model, because benzene partitioning and retardation are not expected to be significantly affected at the ethanol concentrations expected for E10 releases (i.e., <10,000 mg/L) [*Da Silva and Alvarez*, 2002; *Powers et al.*, 2001b].

[12] Limitations to benzene biodegradation rates caused by MFD are incorporated into GSIM through the variable f_S,

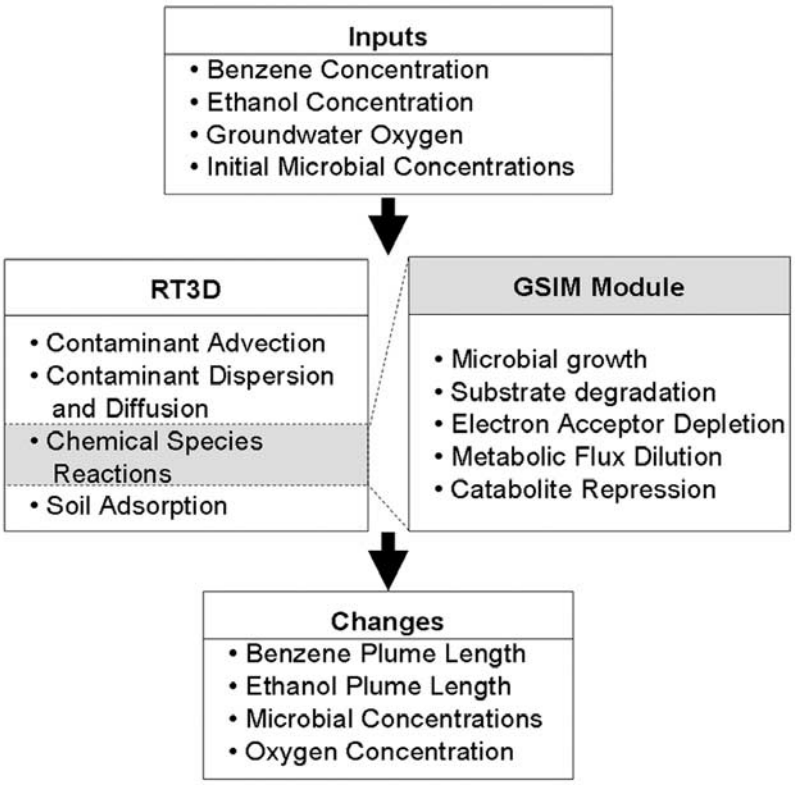

Figure 1. Processes considered by RT3D and GSIM for the simulation of benzene and ethanol fate and transport.

which is calculated as the aqueous concentration of a substrate S (benzene in this case) divided by the total concentration of other dissolved organic species, expressed on a total organic carbon (TOC) basis after excluding biomass:

$$f_S = \frac{S_{TOC}}{T_{TOC}} \tag{2}$$

where f_S is the metabolic flux dilution factor (dimensionless), S_{TOC} is the substrate concentration as total organic carbon (mg/L) and T_{TOC} is the total organic carbon concentration (mg/L). The specific substrate utilization rate of the substrate in the absence of ethanol (U_S, [g/g d]) is multiplied by f_S [*Lovanh and Alvarez*, 2004] to obtain the corrected rate (U_S^*, [g/g d]). That is,

$$U_S^* = f_S \cdot U_S \tag{3}$$

Thus, as the concentration of ethanol increases, f_S decreases, and the specific substrate utilization rate of benzene is increasingly diminished, potentially leading to longer plumes.

[13] Catabolite repression (CR) was modeled as a modulated mechanism in which the induction of a hydrocarbon catabolic gene decreases with increasing concentrations of the repressor (i.e., ethanol) and increases with the relative availability of the inducer (i.e., benzene) in the mixture, as shown by *Lovanh and Alvarez* [2004]. Thus, CR was considered by assuming that U_S^* is proportional to f_S. Recalling that MFD separately implies that U_S^* is also proportional to f_S (equation (3)), a simple (multiplicative) empirical equation was used to combine the effects of MFD and CR [*Lovanh and Alvarez*, 2004]:

$$U_S^* = f_s^2 \cdot U_S \tag{4}$$

[14] Substrate biodegradation is modeled using a system of equations based on multiplicative Monod kinetics that incorporate MFD plus CR (equations (3) and (4)), recognizing that the overall degradation rate (r) is the product of the specific degradation rate (U) and the microbial concentration (X). Thus, degradation rate equations are derived for both aerobic (equation (5)) and anaerobic conditions (limited to methanogenic conditions in the latter case) (equation 6). Oxygen consumption (equation (7)) [*Borden and Bedient*, 1986], aerobic biomass growth (equation (8)) and anaerobic biomass growth (equation (9)) are also considered. All biomass is assumed to be attached in the form of immobile microcolonies that behave as fully penetrated biofilms [*Chen et al.*, 1992], as is the case for at least 99% of subsurface microorganisms [*Harvey et al.*, 1984; *Lehman et al.*, 2001].

[15] The reaction term (R) in equation (1), translates directly into equations (5)–(7), while microbial growth is represented in equations (8) and (9) (variable definitions in Tables 1a, 1b, and 2):

$$r_{S,Aer} = \left[\frac{dS}{dt}\right]_{Aer} = -\frac{f_S^2}{R_S}\left[\frac{\mu_{mS,Aer} X_{Aer}}{Y_{S,Aer}}\left(\frac{S}{K_{S,Aer}+S}\right)\left(\frac{O}{K_O+O}\right)\right] \tag{5}$$

$$r_{S,An} = \left[\frac{dS}{dt}\right]_{An} = -\frac{f_S^2}{R_S}\left[\frac{\mu_{mS,An} X_{An}}{Y_{S,An}}\left(\frac{S}{K_{S,An}+S}\right)\right] \tag{6}$$

Table 1a. Biodegradation Kinetics Model Parameters

Parameter	Value	Reference
	Ethanol Aerobic	
$\mu_{mE,Aer}$, d^{-1}	11.0	*Lovanh et al.* [2002]
$Y_{E,Aer}$, mg/mg	0.5	Based on mix culture aerobic systems [*Heulekian et al.*, 1951]
$K_{E,Aer}$, mg/L	63.1	Calculated using λ[a]
$\lambda_{E,Aer}$, d^{-1}	0.35	*Corseuil et al.* [1998]
	Ethanol Anaerobic	
$\mu_{mE,An}$, d^{-1}	1.10	*Oonge* [1993]
$Y_{E,An}$, mg/mg	0.07	Based on methane fermentation [*Lawrence and McCarty*, 1969]
$K_{E,An}$, mg/L	78.9	Calculated using λ[a]
$\lambda_{E,An}$, d^{-1}	0.200	*Corseuil et al.* [1998]
	Benzene Aerobic	
$\mu_{mB,Aer}$, d^{-1}	3.2	*Alvarez et al.* [1991]
$Y_{B,Aer}$, mg/mg	0.39	*Alvarez et al.* [1991]
$K_{B,Aer}$, mg/L	7.6	*Alvarez et al.* [1991]
$\lambda_{B,Aer}$, d^{-1}	0.68	*Alvarez et al.* [1991]
	Benzene Anaerobic	
$\mu_{mB,An}$, d^{-1}	0.3	*Ulrich and Edwards* [2003]
$Y_{B,An}$, mg/mg	0.05	Based on methane fermentation [*O'Rourke*, 1968]
$K_{B,An}$, mg/L	21.6	Calculated using λ[a]
$\lambda_{B,An}$, d^{-1}	0.003	*Aronson and Howard* [1997]

[a]Here λ is the first-order degradation rate coefficient. Values were estimated on the basis of the relationship $\lambda = (\mu X/YK_s)$ [*Alvarez and Illman*, 2006] for initial microbial populations.

$$r_O = \frac{dO}{dt} = \left[r_{S,Aer} F_S\right] \tag{7}$$

$$r_{X,Aer} = \frac{dX_{Aer}}{dt} = -\left[r_{S,Aer} Y_{S,Aer}\right]\left(1 - \frac{\eta_{bio}}{\gamma \cdot n}\right) - b_{Aer} X_{Aer} \tag{8}$$

$$r_{X,An} = \frac{dX_{An}}{dt} = -\left[r_{S,An} Y_{S,An}\right]\left(1 - \frac{\eta_{bio}}{\gamma \cdot n}\right) - b_{An} X_{An} \tag{9}$$

where $\mu_{mS,Aer}$ and $\mu_{mS,An}$ are the maximum specific growth rate of aerobic biomass and anaerobic biomass respectively (d^{-1}), $Y_{S,Aer}$ and $Y_{S,An}$ are the aerobic and anaerobic biomass yield coefficients (g biomass/g substrate), and $K_{S,Aer}$ and $K_{S,An}$ are the half-saturation coefficients of the substrate under aerobic and anaerobic metabolism (mg/L). Equations (5) and (6) describe the loss of substrates due to aerobic and anaerobic biodegradation, which is conservatively assumed to occur only in the liquid phase. Catabolite repression and metabolic flux dilution, as well as soil adsorption, are accounted for through the f_S terms and retardation factor R_S. Equation (7) describes the loss of oxygen by aerobic biodegradation processes. Equations (8) and (9), describe aerobic and anaerobic biomass growth (limited to methanogenic growth for E10 release scenarios). The new values of substrate, electron acceptor, and biomass concentrations at the end of each time step in each grid block are then returned to RT3D as initial values for the subsequent time step. This process is repeated for each time step of simulation.

[16] Since both aerobic and anaerobic (methanogenic) processes are considered, the change from aerobic to anaerobic conditions is simulated by implementing a "switching" function [*Widdowson et al.*, 1988]. This function uses an empirical factor $I_{An,O}$ that gradually initiates anaerobic metabolism as oxygen concentration decreases:

$$\left(\frac{I_{An,O}}{I_{An,O} + O}\right) \tag{10}$$

where O is the oxygen concentration. The anaerobic substrate utilization rate is multiplied by the switching function for simulation of anaerobic biodegradation to limit anaerobic metabolism when oxygen is present.

[17] GSIM also provides mechanisms to control total microbial biomass through a maximum pore space utilization factor γ. The biomass growth expressions of equations (7) and (8) are multiplied by a term to limit the volume of the biomass [*de Blanc et al.*, 1996]:

$$\left(1 - \frac{\eta_{bio}}{\gamma \cdot n}\right) \tag{11}$$

where η_{bio} is the total biomass saturation (volume of biomass per volume of pore space) and n is the total porosity. The value of η_{bio} is calculated as

$$\eta_{bio} = \frac{X_{Aer,T} + X_{An,T}}{\rho} \tag{12}$$

where ρ = biomass density (mass of cells/volume of biomass), $X_{Aer,T}$ is the total aerobic biomass concentration (mg/L), and $X_{An,T}$ is the total anaerobic biomass concen-

Table 1b. Additional Biodegradation Model Parameters

Parameter	Value	Reference
Maximum pore space utilization factor γ	0.20	*Vandevivere et al.* [1995]; *Thullner et al.* [2002]
b_{Aer}, d^{-1}	0.2	Based on mix culture aerobic systems [*McCarty and Brodersen*, 1962]
b_{An}, d^{-1}	0.03	Based on methane fermentation [*Lawrence and McCarty*, 1969]
K_O, mg/L	0.21	*Fritzsche* [1994]
F_E, mg/mg	1.27	Stoichiometry
F_B, mg/mg	3.07	Stoichiometry
$X_{Aer,E}$ aerobic ethanol degraders, initial, mg/L	1	*Chen et al.* [1992]
$X_{An,E}$ anaerobic ethanol degraders, initial, mg/L	0.1	Assumed 10% of aerobes
$X_{Aer,b}$ aerobic benzene degraders, initial, mg/L	0.1	Assumed 10% of total
$X_{An,b}$ Anaerobic benzene degraders, initial, mg/L	0.001	Assumed 1% of aerobes
Biofilm density, mg/L	10^5	High-density biofilm [*Freitas dos Santos and Livingston*, 1995; *Zhang and Bishop*, 1994]

Table 2. Hydrogeophysical Model Parameters

Parameter	Value	Reference
	Hydrogeology	
Hydraulic conductivity K	3.0 m/d	Fine-medium sand, LNAST soils database[a]
Hydraulic gradient i	0.003 m/m	*Newell et al.* [1996]
Darcy water velocity v	0.9 cm/d	Fine-medium sand, LNAST soils database[a]
Total porosity n	0.3	*Newell et al.* [1996]
Groundwater dissolved oxygen O	6 mg/L	*Newell et al.* [1996]
Pore space utilization factor γ	0.2	*Vandevivere et al.* [1995]; *Thullner et al.* [2002]
	Dispersivity	
Longitudinal	7 m	*Newell et al.* [1996][b]
Transverse	0.7 m	
	Adsorption	
Soil bulk density ρ_b	1.7 kg/L	*Newell et al.* [1996]
Partitioning coefficient, ethanol, K_{dE}	0.001 L/kg	
Retardation factor, ethanol, R_E	1.01	Calculated, $R_E = 1 + \rho_b K_{dE}/n$
Partitioning coefficient, benzene, K_{dB}	0.095 L/kg	
Retardation factor, benzene, R_B	1.54	Calculated, $R_B = 1 + \rho_b K_{dB}/n$
	General Simulation	
Modeled area length	300 m	
Modeled area width	80 m	
X space discretization	75 units	
Y space discretization	100 units	
Cell width	0.8 m	
Cell length	4 m	
Simulation time	30 years	
Time step	0.02	

[a] *Huntley and Beckett* [2002].

tration (mg/L). At low biomass concentrations, the growth limiting expression of equation (11) has a negligible effect on biomass growth and substrate utilization rates because the biomass occupies a relatively small volume of the total pore space. As the biomass increases, the growth limiting expression (equation (11)) approaches zero.

2.3. Microbial Population Shifts

[18] Simultaneous benzene and ethanol utilization was implemented as four different degradation processes involving four separate microbial populations: X_1, aerobic ethanol degraders; X_2, aerobic ethanol and benzene degraders; X_3, anaerobic ethanol degraders; and X_4, anaerobic ethanol and benzene degraders. This division of biomass accounts for the fact that all microbial populations (X_1, X_2, X_3 and X_4) can degrade ethanol, but that only a subgroup of these can degrade benzene (X_2 and X_4). Thus, some benzene degraders can grow fortuitously on ethanol. However, ethanol can stimulate the growth of other bacteria faster than hydrocarbon degraders, which decreases the relative abundance of benzene degraders [*Da Silva and Alvarez*, 2002; *Capiro et al.*, 2007]. This phenomenon is coined here as "genotypic dilution." All biomass in our model is assumed to be attached in the form of immobile microcolonies that behave as fully penetrated biofilms [*Chen et al.*, 1992], which is the case for at least 99% of subsurface microorganisms [*Harvey et al.*, 1984; *Lehman et al.*, 2001].

[19] The pertinent biodegradation and growth equations specific to this system are described below and the variables and their assigned values are listed in Tables 1a, 1b, and 2 (Subscript $S = B$ for benzene and $S = E$ for ethanol):

Biodegradation of ethanol

$$
\begin{aligned}
r_E &= \left[\frac{dE}{dt}\right] = -\frac{f_E}{R_E}\left(r_{E,1} + r_{E,2} + r_{E,3} + r_{E,4}\right)\\
r_{E,1} &= \frac{\mu_{E,Aer1} X_1}{Y_{E,Aer1}}\left(\frac{E}{K_{E,Aer1} + E}\right)\left(\frac{O}{K_O + O}\right)(aerobic)\\
r_{E,2} &= \frac{\mu_{E,Aer2} X_2}{Y_{E,Aer2}}\left(\frac{E}{K_{E,Aer2} + E}\right)\left(\frac{O}{K_O + O}\right)(aerobic)\\
r_{E,3} &= \frac{\mu_{E,An1} X_3}{Y_{E,An1}}\left(\frac{E}{K_{E,An1} + E}\right)\left(\frac{I_{An,O}}{I_{An,O} + O}\right)(anaerobic)\\
r_{E,4} &= \frac{\mu_{E,An2} X_4}{Y_{E,An2}}\left(\frac{E}{K_{E,An2} + E}\right)\left(\frac{I_{An,O}}{I_{An,O} + O}\right)(anaerobic)
\end{aligned}
\tag{13}
$$

Biodegradation of benzene

$$
\begin{aligned}
r_B &= \left[\frac{dB}{dt}\right] = -\frac{f_B^2}{R_B}\left(r_{B,2} + r_{B,4}\right)\\
r_{B,2} &= \frac{\mu_{B,Aer} X_2}{Y_{B,Aer}}\left(\frac{B}{K_{B,Aer} + B}\right)\left(\frac{O}{K_O + O}\right)(aerobic)\\
r_{B,4} &= \frac{\mu_{B,An} X_4}{Y_{B,An}}\left(\frac{B}{K_{B,An} + B}\right)\left(\frac{I_{An,O}}{I_{An,O} + O}\right)(anaerobic)
\end{aligned}
\tag{14}
$$

Oxygen consumption

$$
r_O = \frac{dO}{dt} = \left[r_{E,1} F_E + r_{E,2} F_E + r_{B,2} F_B\right] \tag{15}
$$

Aerobic ethanol degraders (X_1) growth

$$r_{X,1} = \frac{dX_1}{dt} = -\left[r_{E,1} Y_{E,Aer1}\right]\left(1 - \frac{\eta_{bio}}{\gamma n}\right) - b_{Aer} X_1 \quad (16)$$

Aerobic ethanol and benzene degraders (X_2) growth

$$r_{X,2} = \frac{dX_2}{dt} = -\left[r_{E,2} Y_{E,Aer2} + r_{B,2} Y_{B,Aer}\right]\left(1 - \frac{\eta_{bio}}{\gamma n}\right) - b_{Aer} X_2 \quad (17)$$

Anaerobic ethanol degraders (X_3) growth

$$r_{X,3} = \frac{dX_3}{dt} = -\left[r_{E,3} Y_{E,An1}\right]\left(1 - \frac{\eta_{bio}}{\gamma n}\right) - b_{An} X_3 \quad (18)$$

Anaerobic ethanol and benzene degraders (X_4) growth

$$r_{X,4} = \frac{dX_4}{dt} = -\left[r_{E,4} Y_{E,An2} + r_{B,4} Y_{B,An}\right]\left(1 - \frac{\eta_{bio}}{\gamma n}\right) - b_{An} X_4 \quad (19)$$

2.4. General Substrate Interaction Module

[20] GSIM (supplemental material[1]) incorporates the biodegradation equations presented above, which comprise a system of ordinary differential equations (ODEs) that must be solved at each grid block and each time step after the advection and dispersion terms are calculated by RT3D. The resulting ODEs are solved in RT3D using reaction solvers contained in MT3D [*Zheng*, 1990] or using a custom module, in this case, GSIM. Equations (1)–(6) are implemented and solved by GSIM to calculate microbial growth, substrate degradation and electron donor consumption.

[21] Numerical stability of the combined flow and biodegradation system simulation was ensured by applying the Peclet and Courant convergence and stability criteria to the model. These criteria affect the time step Δt and the space discretization of the grid Δx in RT3D, respectively, and minimize the numerical errors due to round off and truncation of derivatives that occur when replaced by finite differences [*Holzbecher and Sorek*, 2005]. The criteria are

Peclet number criterion

$$P_e = \frac{\bar{v} \cdot \Delta x}{D} \leq 2 \quad (20)$$

Courant number criterion

$$C_r = \frac{\bar{v} \cdot \Delta t}{\Delta x} \leq 1 \quad (21)$$

where P_e is the Peclet stability number (dimensionless), C_r is the Courant stability number (dimensionless), $\bar{v}$ is the average linear flow velocity (m/d), Δt is the time step difference (d), Δx is the spatial step difference (m) and D is the coefficient of hydrodynamic dispersion (m^2/d).

2.5. Model Verification and Calibration

[22] GISM was tested by comparing the output of MODFLOW/RT3D/GSIM with BIOSCREEN [*Newell et al.*, 1996] applied to a field study, Keesler Air Force Base (SWMU 66), with extensive data characterization. GSIM simulations considered flow and transport of BTEX, under the same set of parameters as BIOSCREEN, and biodegradation parameters from the literature, maintaining the approximate first-order degradation coefficients used in that model. Hydrogeological data and biokinetic parameters used to model this site are readily available from the user's manual [*Newell et al.*, 1996]. This simulation was used to calibrate the domain simulation parameters for stability (cell size and time step), and to verify the behavior of the system of equations of the model under known conditions and results.

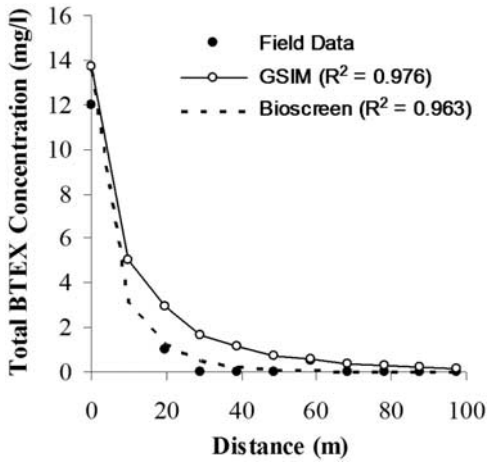

Figure 2. Centerline BTEX concentration as a function of distance for a constant source (Keesler AFB data).

[23] The simulation was run for 6 years, and the BTEX source concentration was simulated as a constant concentration of 13.7 mg/L [*Newell et al.*, 1996]. Data was compared with a first-order model, thus, values of biokinetic parameters for GSIM were manipulated to simulate first-order reactions. Figure 2 compares the output of both models and field data from sampling wells. The concentration profiles of the two are similar, and with an R^2 of 0.98, the GSIM module fits the data slightly better than BIOSCREEN (R^2 of 0.96).

[24] Validation of the microbial kinetics module was done by comparing simulated benzene and ethanol concentrations with results from laboratory microcosm studies by *Hunt et al.* [1997]. The simulations matched ethanol data with an R^2 of 0.96, and benzene data with a R^2 of 0.94 (supplemental material). Thus, model outputs for benzene degradation in the presence of ethanol closely matched laboratory data.

2.6. Initial, Boundary, and Domain Conditions for Simulations

[25] The domain for all model simulations in this paper consists of a single (2-D), 3-m thick layer that is 80 m wide by 300 m long. A constant seepage velocity of 0.9 cm/d was created using constant boundary conditions at the two ends of the model domain (H = 2 m measured from bottom on left boundary, H = 1.4 m measured from bottom on right boundary), and the top and bottom of the domain were specified as no-flow boundaries. Other properties of the model domain are shown in Table 2. Variables defined for these simulations include three mobile species dissolved in groundwater (i.e., (1) ethanol, (2) benzene, and (3) oxygen), and four immobile species attached to aquifer material (i.e.,

[1] Auxiliary materials are available in the HTML. doi:10.1029/2007WR006184.

(4) aerobic ethanol degraders, (5) anaerobic ethanol degraders, (6) aerobic benzene degraders, and (7) anaerobic benzene degraders).

[26] All simulations were based on the same set of microbial kinetic and hydrogeological parameters. Tables 1a and 1b list the microbial kinetic parameters used. The initial dissolved oxygen concentration was set at 6 mg/L, and groundwater entering the model domain contained this same dissolved oxygen concentration. For anaerobic processes, the system was assumed to become strongly anaerobic (methanogenic conditions), which commonly occurs as a result of the rapid depletion of thermodynamically more favorable electron acceptors [*Da Silva and Alvarez*, 2002]. Initial microbial concentrations for all ethanol aerobic populations and benzene aerobic populations on the domain were set to 1 mg/L ($\sim 10^6$ cells/g soil) and 0.1 mg/L ($\sim 10^5$ cells/g soil), respectively. Maximum pore space occupation by microbial species during growth was set at 20%, corresponding to a porosity reduction of 80% of the initial value [*Vandevivere et al.*, 1995; *Thullner et al.*, 2002]. Ethanol anaerobic population and benzene anaerobic population initial concentrations were set to 0.1 mg/L ($\sim 10^5$ cells/g soil) and 0.001 mg/L ($\sim 10^3$ cells/g soil), respectively.

2.7. Source Zone Concentrations

[27] Two types of source zones were simulated: a constant concentration source and a decreasing concentration source. For both release scenarios, benzene and ethanol in the groundwater were assumed to originate from a spill of nonaqueous phase liquid (NAPL). For the constant concentration scenario, an ethanol concentration of 1,000 mg/L [*Wilson and Adair*, 2006] and a benzene concentration of 10 mg/L were assumed to exist at the source as a result of a relatively large NAPL release.

[28] For the decreasing source concentration scenario, concentrations of benzene and ethanol in the groundwater directly in contact with the source NAPL were estimated using the American Petroleum Institute's (API) LNAPL Dissolution and Transport Screening Tool (LNAST) model [*Huntley and Beckett*, 2002]. LNAST provides water phase concentrations of gasoline components at the interface between groundwater and LNAPL. To use this output as input for RT3D, we assumed that gasoline constituent concentrations just below the LNAPL/Water interface decrease rapidly to nondetect levels within two to three meters [*Huntley and Beckett*, 2002]. Thus, we used source cell concentrations that represent the average between LNAST output (i.e., the interface value at the top of the source cells) and zero (i.e., the value at the bottom of the source cells). A release of 2,000 kg of an ethanol/benzene mixture (E10) was considered. Spill volume was chosen to match model grid cell size and mass, resulting in a LNAPL spill on a volume 4 m wide by 4.8 m long by 0.79 m thick above groundwater level. Parameters used to estimate source concentrations were those shown in Table 2. The average depth to the top of the LNAPL was considered to be 1.2 m. E10 composition used, in mole fraction, was 0.015 for benzene, 0.172 for ethanol, 0.158 for TEX and 0.824 for other compounds [*Poulsen et al.*, 1991]. LNAST predicted initial ethanol and benzene concentrations at the LNAPL/water interface of 80,000 and 32 mg/L, respectively, decaying over time.

2.8. Model Limitations

[29] Although the GSIM module is very versatile allowing for multiple substrates, biological species and electron acceptors, in this paper we have focused on a simplified case of an E10 spill. The module itself and this implementation have several limitations that are important to highlight: (1) The model currently does not consider cosolvency effects, which can affect the rate of dissolution and sorption for higher ethanol blends (e.g., E85). (2) Microbial activity is assumed to occur attached to the soil matrix. The model does not consider transport of microbial biomass or attachment/detachment kinetics. (3) Substrate degradation is conservatively assumed to occur only in the liquid phase, ignoring potential decay of sorbed contaminants. (4) Although the model can account for an arbitrary number of electron acceptors, oxygen is the only electron acceptor in the simulations (ignoring nitrate-, iron-, and sulfate-reducing pathways), as we have assumed that the large electron acceptor demand exerted by high ethanol concentrations causes a relatively rapid transition to (anaerobic) methanogenic conditions. (5) Only ethanol and benzene have been considered for our E10 release case, and no other gasoline components are evaluated. This greatly speeds simulation times, and under our assumed conditions of highly anaerobic methanogenic conditions, their effects on electron acceptor depletion should be negligible. (6) Total organic carbon (TOC) is assumed to be completely available for degradation processes, and is only used to calculate the metabolic flux dilution factor f_s, not to calculate the specific substrate utilization rate U. (7) The operator splitting solution scheme of the model requires that small time steps (supplemental material) be used in the simulations (<0.005 d) because of convergence and stability issues.

3. Results and Discussion

[30] A sensitivity analysis of the system (supplemental material) was performed to assess the most influential variables involved in the system. The analysis consisted of several different simulations of the ethanol/benzene E10 system, changing one variable at a time by −50% and +50% (or 2 and 4 orders of magnitude in the case of hydraulic conductivity), and then comparing the point elasticity of the benzene centerline plume length after 10 years under each variable. Point elasticity is defined as the percent change of a function (plume length in this case) under a percent change of a variable, $E(f(x)) = (dx/dy)(y/x)$ [*Case and Fair*, 1999]. Results indicate that soil hydraulic parameters: porosity (n), hydraulic conductivity (k) and hydraulic gradient (i), are the most relevant (0.76, 0.86 and 0.55 point elasticity, respectively), consistent with water flow being the primary process involved in the fate and transport of contaminants in groundwater.

[31] Source zone benzene concentration and biofilm density are also important with point elasticities of 0.33 and 0.26 respectively. At benzene concentrations below 1 mg/L, electron acceptor depletion by ethanol increases point elasticity of benzene concentration up to ~0.55. Benzene and ethanol aerobic microbial growth kinetics follow in importance (0.13 to 0.54 elasticity), as they define the rate at which the plume fringe aerobic degra-

Table 3. Simulation Scenarios for Constant Concentration Source Simulations

Scenario	Conditions
Baseline, no ethanol	Only benzene present, considering O_2 consumption during benzene degradation
EAD	Benzene and ethanol, considering O_2 depletion during ethanol degradation
EAD + FG	Benzene and ethanol, with fortuitous growth of benzene degraders
EAD + CR	Considers both O_2 depletion and catabolite repression
EAD + MFD	Considers both O_2 depletion and metabolic flux dilution
EAD + FG + MFD + CR	Considers O_2 depletion, fortuitous growth, metabolic flux dilution and catabolite repression
EAD + MFD + CR + O_2	Considers metabolic flux dilution and catabolite repression, with unlimited O_2 supply.

dation occurs. Benzene and ethanol anaerobic kinetics are third in importance with elasticity up to 0.20; significantly lower because of the low degradation rates of anaerobic processes relative to aerobic degradation. It is interesting to note that none of the values obtained in the analysis is larger than one, which indicates that the system is largely inelastic to changes in a single variable.

[32] The model was used first to evaluate the dissolved benzene groundwater plume from a constant source. Plume length was defined as the distance from the source to the 5 μg/L contour, corresponding to the drinking water MCL (maximum concentration level) for benzene [*U.S. Environmental Protection Agency*, 2003], along the flow direction. Simulated plumes were allowed to reach steady state, which generally occurred after approximately 10 years of simulation. Seven different scenarios (Table 3) were implemented. For both constant concentration and decreasing concentration sources, the MODFLOW/RT3D/GSIM system produced plume lengths within the range reported by *Ruiz-Aguilar et al.* [2003] for plumes from gasoline stations (80 m median and 152 m maximum).

[33] The constant source simulations yielded steady state plumes after ~30 years (Figures 3 and 4). In these simulations, the biochemical oxygen demand exerted by benzene alone near the source was higher than the available dissolved oxygen (as is often the case in contaminated sites), leading to anaerobic conditions in the center of the plume. Fortuitous growth of benzene degraders on ethanol contributed to higher anaerobic degradation rates and resulted in a decrease of 48% in benzene plume length (without MFD and catabolite repression). Benzene/ethanol simulations with no substrate interactions considered resulted in a 7% plume length increase due to ethanol-driven oxygen depletion. Catabolite repression increased benzene plume length by 49%, compared to a 123% increase for MFD. Metabolic Flux dilution was thus the most influential plume elongation mechanism for this constant E10 release scenario.

[34] Simulations considering a decreasing source (Figure 5) show smaller increases in the maximum benzene plume length due to the presence of ethanol and a sharp decline in plume length once ethanol is completely depleted in the system. The baseline scenario with benzene alone reached a maximum length of 35.5 m. In the presence of ethanol, electron acceptor depletion increased plume length by 13%, catabolite repression by 23% and MFD by 46%. All substrate interactions resulted in a combined plume length increase of 22%. Metabolic flux dilution was thus the most influential factor in this E10 release scenario.

[35] Regarding microbial populations, when dissolved oxygen was allowed to deplete, as is the case under natural attenuation conditions, anaerobic microorganisms reached

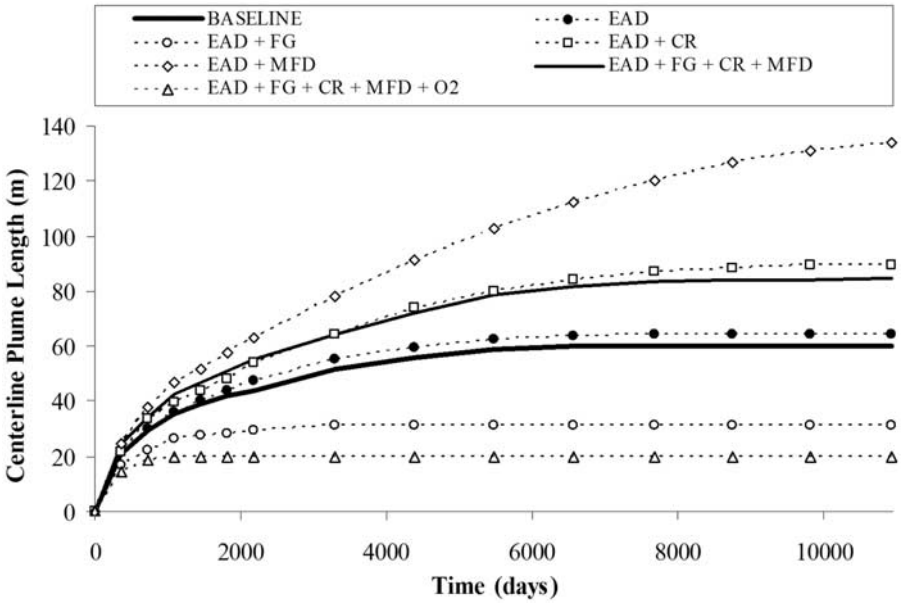

Figure 3. Influence of various inhibitory mechanisms (dissolved oxygen depletion, metabolic flux dilution (MFD) and catabolite repression (CR)) on the elongation of a simulated benzene plume emanating from a constant benzene/ethanol source. Model parameters are given in Tables 1a, 1b, and 2.

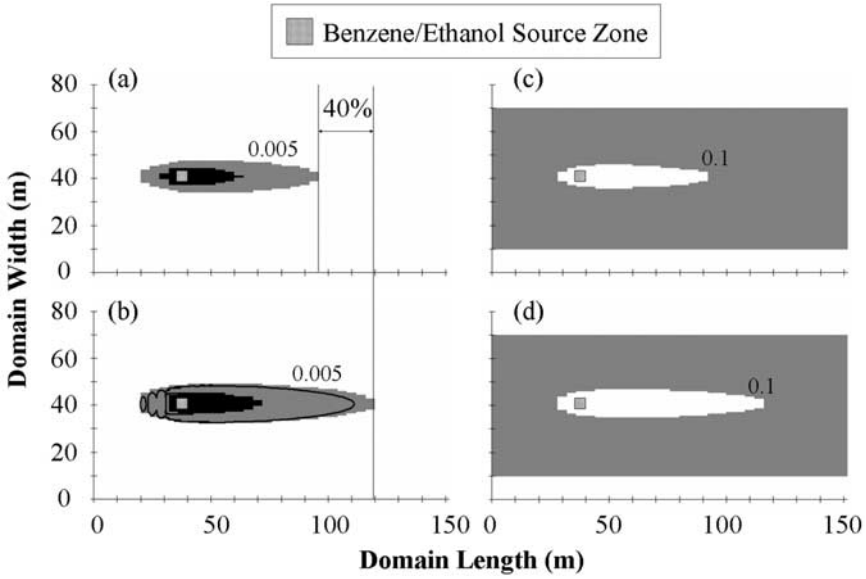

Figure 4. The 30-year, steady state benzene and ethanol plumes, showing the effects of (a) baseline with source zone benzene concentration of 10 mg/L (1 and 0.005 mg/L contours), (b) 40% benzene plume length increase with source zone ethanol concentration of 1000 mg/L (1 and 0.005 mg/L benzene contours and 0.005 mg/L ethanol (solid line)), (c) anaerobic shadow caused by benzene degradation (0.1 mg/L dissolved oxygen contour), and (d) anaerobic shadow caused by ethanol plus benzene degradation (0.1 mg/L dissolved oxygen contour).

consistently higher concentrations than aerobic populations. Figure 6 shows the spatial distribution of microbial populations after 30 years of simulation (steady state), with anaerobic population thriving in the anaerobic source zone, and some aerobic activity still taking place on the plume fringes. Anaerobic degradation is the main substrate consumption mechanism at this point in the plume life cycle, while aerobic degradation dominated early in the simulations (<1 year). For constant source simulations, microbial growth associated with the consumption of ethanol increased total microbial populations near the source zone (0.5 m downgradient) from 10^6 to 10^8 cells/g soil (Figure 7), and up to 10^{10} cells/g soil at the source zone, resulting in increased benzene degrader populations (+180%), while decreasing the ratio of benzene degraders to total degraders (25% to 2%). Figure 8 shows that for a decreasing source scenario, total microbial populations decreased faster than benzene degrader populations, resulting in an increase in the ratio of benzene to total degraders during the first ~800 d of simulation, then decreasing until reaching equilibrium at about 1%. This ratio agrees in order of magnitude with previous studies [*Capiro et al.*, 2007]. In

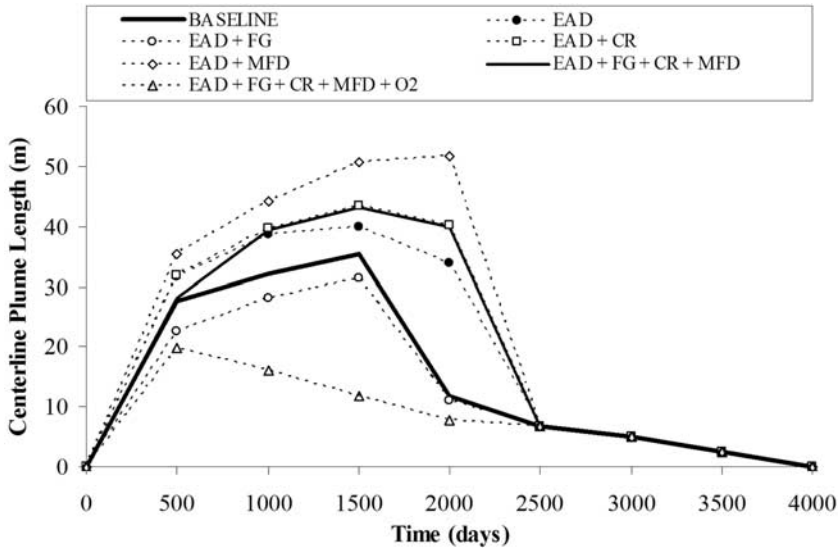

Figure 5. Influence of various inhibitory mechanisms (dissolved oxygen depletion, metabolic flux dilution (MFD), and catabolite repression (CR)) on the elongation of a simulated benzene plume emanating from a decreasing source. Model parameters are given in Tables 1a, 1b, and 2.

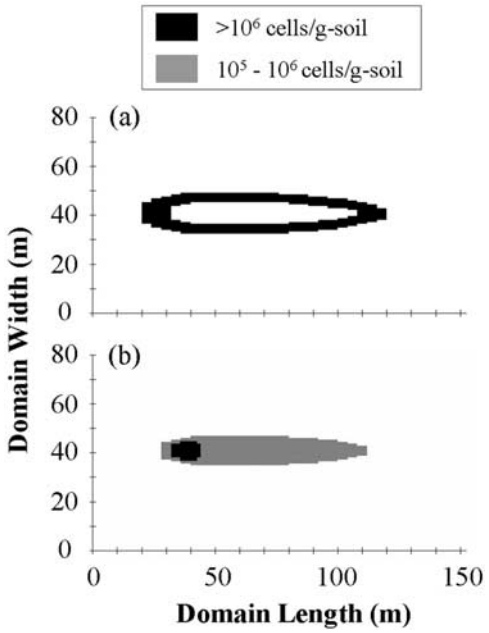

Figure 6. The 30-year, steady state microbial concentration contours (cells/g soil): (a) aerobic benzene degraders and (b) anaerobic benzene degraders. Shaded cells indicate populations larger than background concentrations.

both cases, benzene degrader populations were higher with ethanol, while their fractions relative to the total populations were smaller. This reflects that ethanol is a preferred substrate for most microbial communities and that genotypic dilution is taking place.

[36] To illustrate the potential benefits of oxygen addition as a bioremediation technique and discern the potential enhancement of aerobic benzene degradation due to additional growth of benzene degraders on ethanol, an unlimited supply of oxygen was provided to the scenario that considers all substrate interactions (Figures 3 and 5). Simulations with a constant source resulted in a plume length decrease of 67% compared to the baseline without ethanol. Total microbial population reached the highest simulated values, generating an increased degradation potential that offset the elongating effects of negative substrate interactions. When applying an unlimited oxygen supply to the decreasing source simulations, benzene plume length decreased by 44%. However, the high oxygen demand exerted by typically high ethanol concentrations may make aerobic stimulation a prohibitively expensive alternative.

4. Conclusions

[37] A custom reaction numerical solver for RT3D (called GSIM) was developed to evaluate the effects of ethanol on benzene plume dynamics, and to investigate the influence of substrate interactions not previously simulated such as dilution of benzene metabolic flux and catabolite repression. The GSIM model results show that the presence of ethanol in E10 can cause benzene plume elongation by up to 40%, which agrees with previous statistical studies of benzene/ethanol plume lengths [*Ruiz-Aguilar et al.*, 2003]. Both constant source and decreasing sources were evaluated, and simulations assuming a decreasing source yielded a lower degree of plume elongation (22%) relative to constant source conditions. For low benzene concentrations (<1 mg/L), oxygen depletion during ethanol degradation was the principal mechanism hindering benzene natural attenuation. For higher benzene concentrations (exerting an oxygen demand higher than the available dissolved oxygen), metabolic flux dilution was the dominant plume elongation mechanism.

[38] In all simulations, ethanol stimulated an increase in microbial populations (including those that degrade benzene), which offset negative substrate interactions, although the relative abundance of benzene degraders decreased (genotypic dilution). Oxygen depletion during ethanol degradation was the principal mechanism hindering benzene natural attenuation, followed by metabolic flux dilution. When oxygen is not limiting, model simulations showed

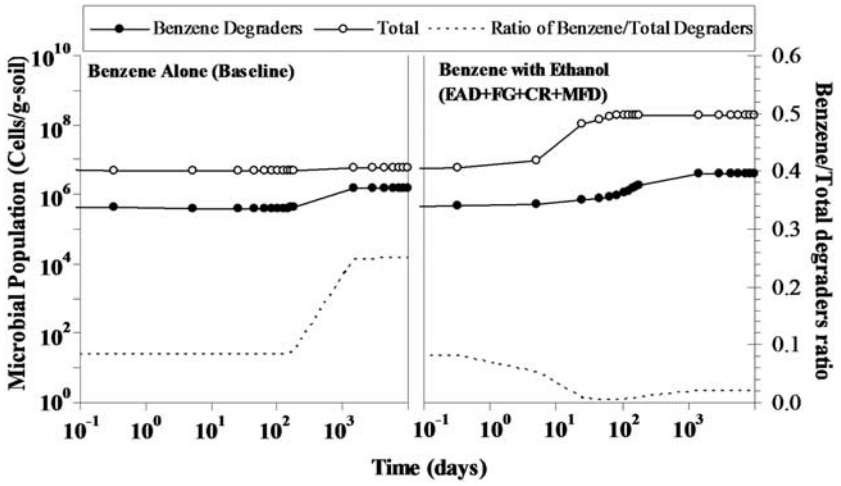

Figure 7. Influence of various inhibitory mechanisms (dissolved oxygen depletion, metabolic flux dilution (MFD), and catabolite repression (CR)) on benzene degraders and total microbial populations (0.1 m downgradient from source) for a benzene/ethanol constant source. Model parameters are given in Tables 1a, 1b, and 2.

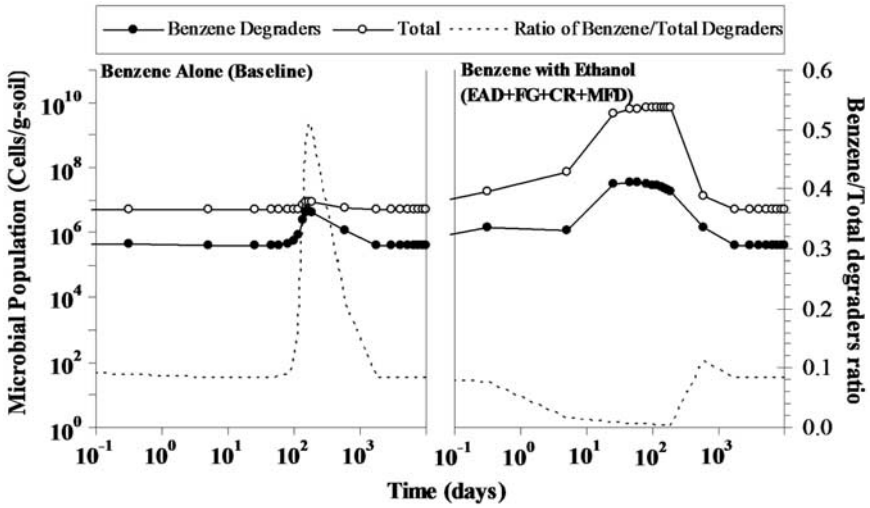

Figure 8. Influence of various inhibitory mechanisms (dissolved oxygen depletion, metabolic flux dilution (MFD), and catabolite repression (CR)) on benzene degraders and total microbial populations (0.1 m downgradient from source) for a decreasing source. Model parameters are given in Tables 1a, 1b, and 2.

that microbial growth on ethanol could offset negative substrate interactions and enhance benzene degradation, resulting in shorter plumes.

[39] This model has some limitations that include ignoring cosolvency effects, assuming that oxygen is the only electron acceptor prior to rapid transition to methanogenic conditions, not considering alkylbenzenes and other gasoline components, and assuming complete availability of total organic carbon for degradation processes. Despite these limitations, this model contributes valuable insight into microbial processes that influence the fate and transport of benzene in the presence of ethanol, and may be a useful tool for assessing the risks of groundwater contamination by E10 fuel.

[40] **Acknowledgments.** The authors wish to thank the U.S. Environmental Protection Agency (grant RD82815602) and the American Petroleum Institute (API) for their support and contributions to this project.

References

Alvarez, P. J. J., and W. A. Illman (2006), *Bioremediation and Natural Attenuation: Process Fundamentals and Mathematical Models*, John Wiley, Hoboken, N. J.

Alvarez, P. J. J., P. J. Anid, and T. M. Vogel (1991), Kinetics of aerobic biodegradation of benzene and toluene in sandy aquifer material, *Biodegradation*, *2*, 43–51, doi:10.1007/BF00122424.

Aronson, D., and P. H. Howard (1997), Anaerobic biodegradation of organic chemicals in groundwater: A summary of field and laboratory studies, report, Environ. Sci. Cent., Syracuse Res. Corp., New York.

Borden, R. C., and P. B. Bedient (1986), Transport of dissolved hydrocarbons influenced by reaeration and oxygen limited biodegradation: 1. Theoretical development, *Water Resour. Res.*, *22*(13), 1973–1982, doi:10.1029/WR022i013p01973.

Capiro, N. L., B. P. Stafford, W. G. Rixey, P. B. Bedient, and P. J. J. Alvarez (2007), Fuel-grade ethanol transport and impacts to groundwater in a pilot-scale aquifer tank, *Water Res.*, *41*(3), 656–664, doi:10.1016/j.watres.2006.09.024.

Case, K. E., and R. C. Fair (1999), *Principles of Economics*, 5th ed., Prentice-Hall, Upper Saddle River, N. J.

Chen, Y., L. M. Abriola, P. J. J. Alvarez, P. J. Anid, and T. M. Vogel (1992), Modeling transport and biodegradation of benzene and toluene in sandy aquifer material: Comparisons with experimental measurements, *Water Resour. Res.*, *28*(7), 1833–1847, doi:10.1029/92WR00667.

Clement, T. P., Y. Sun, B. S. Hooker, and J. N. Petersen (1998), Modeling multi-species reactive transport in groundwater aquifers, *Ground Water Monit. Rem.*, *18*(2), 79–92, doi:10.1111/j.1745-6592.1998.tb00618.x.

Clement, T. P., C. D. Johnson, Y. Sun, G. M. Klecka, and C. Bartlett (2000), Natural attenuation of chlorinated solvent compounds: Model development and field-scale application, *J. Contam. Hydrol.*, *42*, 113–140, doi:10.1016/S0169-7722(99)00098-4.

Corseuil, H. X., C. Hunt, R. Ferreira dos Santos, and P. J. J. Alvarez (1998), The influence of the gasoline oxygenate ethanol on aerobic and anaerobic BTX biodegradation, *Water Res.*, *32*, 2065–2072, doi:10.1016/S0043-1354(97)00438-7.

Da Silva, M. L. B., and P. J. J. Alvarez (2002), Effects of ethanol versus MTBE on BTEX migration and natural attenuation in aquifer columns, *J. Environ. Eng.*, *128*(9), 862–867, doi:10.1061/(ASCE)0733-9372(2002)128:9(862).

de Blanc, P. C., G. E. Speitel Jr., and D. C. McKinney (1996), A three-dimensional, multi-component model of non-aqueous phase liquid flow and biodegradation in porous media, paper presented at Conference on Non-Aqueous Phase Liquids in the Subsurface Environment: Assessment and Remediation, Am. Soc. of Civ. Eng., Washington, D. C., Nov.

Egli, T., U. Lendenmann, and M. Snozzi (1993), Kinetics of microbial growth with mixtures of carbon sources, *Antonie Van Leeuwenhoek*, *63*, 289–298, doi:10.1007/BF00871224.

Freitas dos Santos, L. M., and A. G. Livingston (1995), Membrane-attached biofilms for VOC wastewater treatment I: Novel in situ biofilm thickness measurement technique, *Biotechnol. Bioeng.*, *47*(1), 82–89.

Fritzsche, C. (1994), Degradation of pyrene at low defined oxygen concentrations by a *mycobacterium* sp, *Appl. Environ. Microbiol.*, *60*(5), 1687–1689.

Groves, F. R., Jr. (1988), Effect of cosolvents on the solubility of hydrocarbons in water, *Environ. Sci. Technol.*, *22*(3), 282–286, doi:10.1021/es00168a007.

Harbaugh, A. W., E. R. Banta, M. C. Hill, and M. G. McDonald (2000), MODFLOW-2000, the U.S. Geological Survey modular ground-water model—User guide to modularization concepts and the ground-water flow process, *U.S. Geol. Surv. Open File Rep.*, *00-92*.

Harvey, R. W., R. L. Smith, and L. George (1984), Effect of organic contamination upon microbial distributions and heterotrophic uptake in a Cape Cod, Mass. aquifer, *Appl. Environ. Microbiol.*, *48*(6), 1197–1202.

Heermann, S. E., and S. E. Powers (1996), The dissolution of BTEX compounds from oxygenated gasoline, in *American Chemical Society Division of Environmental Chemistry Preprints of Extended Abstracts*, *36*(1), 221–224.

Heulekian, H., H. E. Orford, and R. Manganelli (1951), Factors affecting the quantity of sludge production in the activated sludge process, *Sewage Ind. Wastes*, *23*, 945–958.

Holzbecher, E., and S. Sorek (2005), Numerical models of groundwater flow and transport, in *Encyclopedia of Hydrological Sciences*, part 13,

vol. 4, edited by M. G. Anderson, pp. 2001–2144, John Wiley, Hoboken, N. J.

Hunt, C. S., R. Ferreira dos Santos, H. X. Corseuil, and P. J. J. Alvarez (1997), Effect of ethanol on aerobic BTX degradation, in *In Situ and Onsite Bioremediation*, vol. 4, edited by B. C. Alleman and A. L. Leeson, pp. 49–54, Battelle, Columbus, Ohio.

Huntley, D., and G. D. Beckett (2002), Evaluating hydrocarbon removal from source zones and its effect on dissolved plume longevity and magnitude, *Publ. 4715*, 275 pp., Am. Pet. Inst., Washington, D. C.

Lawrence, A. W., and P. L. McCarty (1969), Kinetics of methane fermentation in anaerobic treatment, *J. Water Pollut. Control Fed.*, *41*(2), R1–R17, Feb.

Lehman, R. M., F. S. Colwell, and G. A. Bala (2001), Attached and unattached microbial communities in a simulated basalt aquifer under fracture- and porous-flow conditions, *Appl. Environ. Microbiol.*, *67*(6), 2799–2809, doi:10.1128/AEM.67.6.2799-2809.2001.

Lovanh, N., and P. J. J. Alvarez (2004), Effect of ethanol, acetate, and phenol on toluene degradation activity and *tod-lux* expression in *Pseudomonas putida* TOD102: Evaluation of the metabolic flux dilution model, *Biotechnol. Bioeng.*, *86*(7), 801–808, doi:10.1002/bit.20090.

Lovanh, N., C. S. Hunt, and P. J. J. Alvarez (2002), Effect of ethanol on BTEX biodegradation kinetics: Aerobic continuous culture experiments, *Water Res.*, *36*, 3739–3746, doi:10.1016/S0043-1354(02)00090-8.

Lu, G., T. P. Clement, C. Zheng, and T. H. Wiedemeier (1999), Natural attenuation of BTEX compounds: Model development and field-scale application, *Ground Water*, *37*(5), 707–717, doi:10.1111/j.1745-6584.1999.tb01163.x.

Madigan, J. T., J. M. Martinko, and J. Parker (2000), *Brock Biology of Microorganisms*, 9th ed., Prentice-Hall, Upper Saddle River, N. J.

McCarty, P. L., and C. F. Brodersen (1962), Theory of extended aeration activated sludge, *J. Water Pollut. Control Fed.*, *34*, 1095–1103.

McNab, W., S. E. Heermann, and B. Dooher (1999), Screening model evaluation of the effects of ethanol on benzene plume lengths, in *Health and Environmental Assessment of the Use of Ethanol as a Fuel Oxygenate—Report to the California Environmental Policy Council in Response to Executive Order D-5-99*, vol. 4, *Potential Ground and Surface Water Impacts*, *Rep. UCRL-AR-135949*, chap. 4, edited by D. W. Rice and G. Cannon, Lawrence Livermore Natl. Lab., Livermore, Calif.

Molson, J. W., J. F. Barker, E. O. Frind, and M. Schirmer (2002), Modeling the impact of ethanol on the persistence of benzene in gasoline-contaminated groundwater, *Water Resour. Res.*, *38*(1), 1003, doi:10.1029/2001WR000589.

Newell, C. J., R. K. Mcleod, and J. R. Gonzales (1996), BIOSCREEN natural attenuation decision support system, user's manual version 1.3, *Rep. EPA/600/R-96/087*, U.S. Environ. Prot. Agency, Washington, D. C., Aug.

Oonge, Z. I. N. (1993), Primary and secondary substrate interactions in anaerobic systems fed chlorinated aliphatics and glucose or acetate, Ph.D. thesis, Univ. of Iowa, Iowa City, Iowa.

O'Rourke, J. T. (1968), Kinetics of anaerobic treatment at reduced temperatures, Ph.D. dissertation, Stanford Univ., Stanford, Calif.

Poulsen, M., L. Lemon, and J. Barker (1991), Chemical fate and impact of oxygenates in groundwater: Solubility of BTEX from gasoline-oxygenate compounds, *Publ. 4531*, Am. Pet. Inst., Washington, D.C.

Powers, S. E., D. Rice, B. Dooher, and P. J. J. Alvarez (2001a), Will ethanol blended gasoline affect groundwater quality? Using ethanol instead of MTBE as a gasoline oxygenate could be less harmful to the environment, *Environ. Sci. Technol.*, *35*, 24A–30A.

Powers, S. E., C. S. Hunt, S. E. Heermann, H. X. Corseuil, D. Rice, and P. J. J. Alvarez (2001b), The transport and fate of ethanol and BTEX in groundwater contaminated by gasohol, *Crit. Rev. Environ. Sci. Technol.*, *31*(1), 79–123, doi:10.1080/20016491089181.

Ruiz-Aguilar, G. M. L., J. M. Fernandez-Sanchez, S. R. Kane, D. Kim, and P. J. J. Alvarez (2002), Effect of ethanol and methyl-tert-butyl ether on monoaromatic hydrocarbon biodegradation: Response variability for different aquifer materials under various electron-accepting conditions, *Environ. Toxicol. Chem.*, *21*, 2631–2639, doi:10.1897/1551-5028(2002)021<2631:EOEAMT>2.0.CO;2.

Ruiz-Aguilar, G. M. L., K. O'Reilly, and P. J. J. Alvarez (2003), A comparison of benzene and toluene plume lengths for sites contaminated with regular vs. ethanol amended gasoline, *Ground Water Monit. Rem.*, *23*(1), 48–53, doi:10.1111/j.1745-6592.2003.tb00782.x.

Sun, Y., and T. P. Clement (1999), A decomposition method for solving coupled multispecies reactive transport problems, *Transp. Porous Media*, *37*, 327–346.

Sun, Y., J. N. Petersen, T. P. Clement, and B. S. Hooker (1998), Effects of reaction kinetics on predicted concentration profiles during subsurface bioremediation, *J. Contam. Hydrol.*, *31*, 359–372, doi:10.1016/S0169-7722(97)00072-7.

Thullner, M., J. Zeyer, and W. Kinzelbach (2002), Influence of microbial growth on hydraulic properties of pore networks, *Transp. Porous Media*, *49*(1), 99–122, doi:10.1023/A:1016030112089.

Ulrich, A. C., and E. A. Edwards (2003), Physiological and molecular characterization of anaerobic benzene-degrading mixed cultures, *Environ. Microbiol.*, *5*, 92–102, doi:10.1046/j.1462-2920.2003.00390.x.

U.S. Environmental Protection Agency (2003), National primary drinking water standards, *Rep. 816-F-03-016*, Washington, D. C., June.

Vandevivere, P., P. Baveye, D. Sanchez de Lozada, and P. De Leo (1995), Microbial clogging of saturated soils and aquifer materials: Evaluation of mathematical models, *Water Resour. Res.*, *31*(9), 2173–2180, doi:10.1029/95WR01568.

Widdowson, M. A., F. J. Molz, and L. D. Benefield (1988), A numerical transport model for oxygen- and nitrate-based respiration linked to substrate and nutrient availability in porous media, *Water Resour. Res.*, *24*(9), 1553–1565, doi:10.1029/WR024i009p01553.

Wilson, J., and C. Adair (2006), The environmental consequences of a release of ethanol to ground water, paper presented at 2006 Ethanol Workshop, U.S. Environ. Prot. Agency, Hagerstown, Md., 3–4 Oct.

Zhang, T. C., and P. L. Bishop (1994), Density, porosity, and pore structure of biofilms, *Water Res.*, *28*(11), 2267–2277.

Zheng, C. (1990), MT3D: A modular three dimensional transport model for simulation of advection, dispersion and chemical reactions of contaminants in groundwater systems, users manual, U.S. Environ. Prot. Agency, Washington, D. C.

P. J. J. Alvarez (corresponding author), P. B. Bedient, and D. E. Gomez, Department of Civil and Environmental Engineering, Rice University, MS-317, 6100 Main Street, Houston, TX 77005, USA. (alvarez@rice.edu; bedient@rice.edu; degomez@rice.edu)

P. C. de Blanc, GSI Environmental, Inc., 2211 Norfolk, Suite 1000, Houston, TX 77098-4054, USA. (pcdeblanc@gsi-net.com)

W. G. Rixey, Department of Civil and Environmental Engineering, University of Houston, N117 Engineering Building 1, Houston, TX 77204-4003, USA. (wrixey@uh.edu)